Analysis and comparison of multiple features for fault detection and prognostic in ball bearings

Khanh T.P. Nguyen[1], Amor Khlaief[1], Kamal Medjaher[1], Antoine Picot[2], Pascal Maussion[2], Diego Tobon[3], Bertrand Chauchat[3], Regis Cheron[3]

[1] *Toulouse INP, ENIT, 65000 Tarbes, France*

[2] *LAPLACE, Université de Toulouse, CNRS, INP, UPS*

[3] *ALSTOM - 48 Rue Albert Dhalenne, Saint-Ouen, Seine-Saint-Denis, 93400, France*

ABSTRACT

Feature extraction is one of the most important elements in Prognostics and Health Management (PHM) systems. Numerous techniques have been proposed for fault detection, diagnostics and prognostics in ball bearings which are key components of rotating machineries, widely used in the industry. Considering the strengths and weaknesses of these techniques, this paper aims at evaluating and analyzing different features in all three signal processing domains: time, frequency and time-frequency. The crucial indicators related to normal and abnormal cases are extracted from both vibration signals and stator current signals. Then, a new metric is proposed to measure the evolution of these indicators with respect to degradation levels of bearings. The performance of every indicator is analyzed to study which feature(s) is(are) better than other(s) and which feature(s) is(are) the best appropriate for vibration and current signals. These results could be effectively used in future for fault detection, diagnostics and prognostics applications.

1. INTRODUCTION

As most of the failures of rotating machineries are related to the bearings (Zhou et al., 2007), it is necessary to monitor the conditions of these components, detect their anomalies and predict their failures. Numerous papers propose to use vibration signals to monitor the bearing condition because their defects generally produce fault signatures in the machine vibration. Major disadvantage of vibration monitoring is high cost of accelerometers and difficulties when accessing to the machine to install the sensors. On the other hand, numerous studies propose to use electrical signals (current or voltage) for bearing fault detection because their sensors are inexpensive and easy to implement. However, bearing fault signatures do not clearly present in the stator current which sometimes has low signal-to-noise ratio (Zhou et al., 2007). Based on vibration or electrical signals, various feature extraction methods have been proposed for fault detection, diagnostics and prognostics in ball bearings. However, a few articles attempt to assess and compare the performance of these features. In (Tandon, 1994), the authors compared only the vibration parameters (RMS, Peak, Crest factor, power and cepstrum) for bearing condition monitoring. For bearing fault diagnostic, the performance of a set of features extracted from vibration signals was evaluated (Mahamad & Hiyama, 2008) using the ratio of average extern distance between classes to the average intern distance within one class. The authors in (Kappaganthu & Nataraj, 2011) proposed to use the mutual information to evaluate performances of various vibration features for detecting inner and outer race defects in rolling element bearings. However, the proposed approach requires the prior information about the feature probability density function that is not easy and might take high time to evaluate. Then, in (Shukla et al., 2015), the authors introduced an ordering metric, that measures the separability between the normalized feature vectors characterizing healthy and faulty classes to rapidly rank the features extracted from vibration signals in time and frequency domains. On the other hand, for electrical signals, the paper (Knöbel et al., 2015) addressed the fault classification issue using features extracted from current and voltage measurements. The authors proposed to use the modified Fisher-ratio (F-ratio), where the best features are the ones having a small intra class covariance but high inter class covariance, for feature selection.

In summary, the above reported work propose metrics to separately assess the performance of features from vibration and electrical signals. In this paper, we address the question of which feature(s) is(are) the best appropriate for vibration and

current signals. Moreover, the robustness of feature ranking when using numerous sensor sources is also considered. The main contribution of this paper is to propose a simple algorithm of feature ranking. It is simple for prompt evaluation, takes into account the standard deviation of feature and does not depend on the feature units. Thus, it allows comparing heterogeneous features in different domains

We firstly present a brief review of feature extraction methods that could be applied for vibration and current signals in Section 2. A fast, simple, and effective ranking algorithm to access the performance of multiple features for fault detection and prognostics is then developed in Section 3. Next, the comparison and analysis of the performance of the features based on real data acquired from our test bench will be discussed in Section 4. Finally, the conclusion and perspective of this work will be presented in Section 5.

2. FEATURE EXTRACTION METHODS

In this section, we present the common, robustness and effective methods of feature extraction that could be applied for both vibration and current signals. In general, these methods can be classified into three categories: time, frequency, and time-frequency domain.

2.1. Features in time domain

Using directly raw data, signal processing in time domain are classical, fast and simple. They play a critical role for fault detection, diagnostic and prognostic. However, these techniques are not viable for noisy signals. It could require a pretreatment techniques to enhance signals before the evaluation of indicators.

Among features in time domain, the statistical indicators are widely used thanks to their strict relations with incipient bearing damages. In fact, the Mean, Variance, Min, Max, Skewness (SKE) and Kurtosis (KUR) values are evaluated based on vibration and current signals (Shukla et al., 2015). The root mean square (RMS) value is also effective for the detection of a localized bearing default by assessing the power content in the vibration signature (Lei et al., 2016 ; Huang et al., 2017) or the stator current signal (Shukla et al., 2015 ; Alameh et al., 2015). On the other hand, the factors that represent the overall shape of signals, such as the Crest factor (CF), Peak to Peak value (PP), Shape factor (SF), and Impulse factor (IF), are powerful to capture changes in the signal pattern of vibration (Mahamad & Hiyama, 2008) or current signals (Shukla et al., 2015) when anomalies occur. In (Sassi et al., 2006), the authors combine the conventional scalar indicators such as RMS, KUR, CF, and Peak to create new indicators that aim to predict future failures and track defects from the first signs of degradation to the end of life.

2.2. Features in frequency domain

Frequency analysis is a common technique to observe the bearing condition because bearing defects generally generate characteristic frequencies in the vibration and current signals (see Annex for the details of the evaluation of characteristic frequencies).

2.2.1. Features extracted from spectrum analysis.

The Fast Fourier Transform (FFT) is widely used to decompose physical signals into number of discrete frequencies or spectrum of continuous frequencies. After performing FFT, the magnitude values at the characteristic frequencies f_c are used as common indicators for bearing fault detection and diagnostic (Kappaganthu & Nataraj, 2011 ; Harlişca et al., 2013). Other usual indicators that can be used for both vibration and current signal spectrum are the statistical parameters such as RMS, root variance (RV), mean, and median values (Mahamad & Hiyama, 2008 ; Shukla et al., 2015). In (Yu, 2012), a frequency feature called PMM, that is the ratio between the maximal value of FFT magnitudes at the characteristic frequencies and the mean of the entire magnitude frequency value, is used for defect and severity classification and for bearing performance assessment. The authors in (Elbouchikhi et al., 2015) used the spectral kurtosis for mechanical unbalance detection in an induction machine using the stator currents instantaneous frequency.

2.2.2. Features extracted from envelope analysis.

The contact of a bearing localized defect with another surface in bearing will generate multiple repetitive vibration impulses. This leads to a concentration of the energy in narrow band. Therefore, the envelope analysis allows effectively detecting bearing failure in different situations. In fact, the maximal value of the envelope spectrum magnitude is used as an indicator for bearing fault detection in (Mahamad & Hiyama, 2008 ; Shukla et al., 2015). Numerous articles show that the envelope spectrum magnitudes at the characteristic frequencies are powerful to detect and classify the bearing failures (Cong et al., 2012 ; Leite et al., 2015). On the other hand, in (Yu, 2012), the ratio between the maximal value of envelope spectrum magnitudes at the characteristic frequencies and the mean value of the entire magnitudes is also used for bearing diagnostic and degradation assessment.

2.3. Features in time-frequency domain

In order to avoid the non-stationary characteristic of signals, it is necessary to present them into two-dimensional function of time and frequency. Therefore, numerous signal processing techniques in time-frequency domain have been developed in literature.

2.3.1. Features extracted from the short time Fourier transform (STFT).

The STFT firstly decomposes the signals into a set of data within a fixed window length and secondly performs the FT on every data window. Then, the spectrum magnitude at FFT characteristic frequencies is proposed to use as an effective feature for bearing defect diagnostic (Yazici & Kliman, 1999). However, the selection of the fixed window length before performing STFT can strongly affect the method performance. Therefore, the wavelet transform based on variable window length is recommended.

2.3.2. Features extracted from wavelet transform.

Wavelet transform (WT) allows flexibly adapting the resolutions of time and frequencies for signal analysis, e.g. good time and poor frequency resolution at high frequencies and vice-versa. This technique can be divided into three groups: continuous wavelet, discrete wavelet and wavelet packet transform. For bearing fault detection, the features are extracted based on statistical evaluation of the wavelet coefficients (Kompella et al., 2016 ; Deekshit Kompella et al., 2017). On the other hand, features evaluated based on the wavelet energy are also widely used for bearing fault detection using vibration (Yu, 2012) or stator current signals (Knöbel et al., 2015 ; Singh et al., 2014). In (Tobon-Mejia, 2012), the authors propose an effective approach based on the utilization of the WPD and the MoG-HHM for bearing failure prognostics.

2.3.3. Features extracted from Hilbert Huang transform.

As the performance of wavelet analysis method strictly depends on the choice of the mother wavelet, it is suitable to use Hilbert Huang transform (HHT) for analyzing non-stationary signals when we do not have a prior information about the signal shape. The HHT technique includes two phases. Firstly, the input signal is decomposed into a set of intrinsic mode functions (IMFs) using Empirical mode decomposition (EMD). Secondly, the instantaneous frequencies of the IMFs are extracted through Hilbert spectrum analysis (HSA). Therefore, HHT becomes a powerful tool for analyzing and characterizing the signal spectrum in time. For bearing fault detection and diagnostic, the HHT marginal spectrum at characteristic frequencies is proved to be an effective indicator extracted from vibration (Refaat et al., 2013) and stator current signals (Elbouchikhi et al., 2017). This indicator is also powerful for prognostic of bearing failure (Soualhi et al., 2015).

3. FEATURE RANKING

3.1. Feature performance measure

In order to evaluate the performance of the extracted features for fault detection and prognostics, it is necessary to propose a new measure that can satisfy the following requirements:

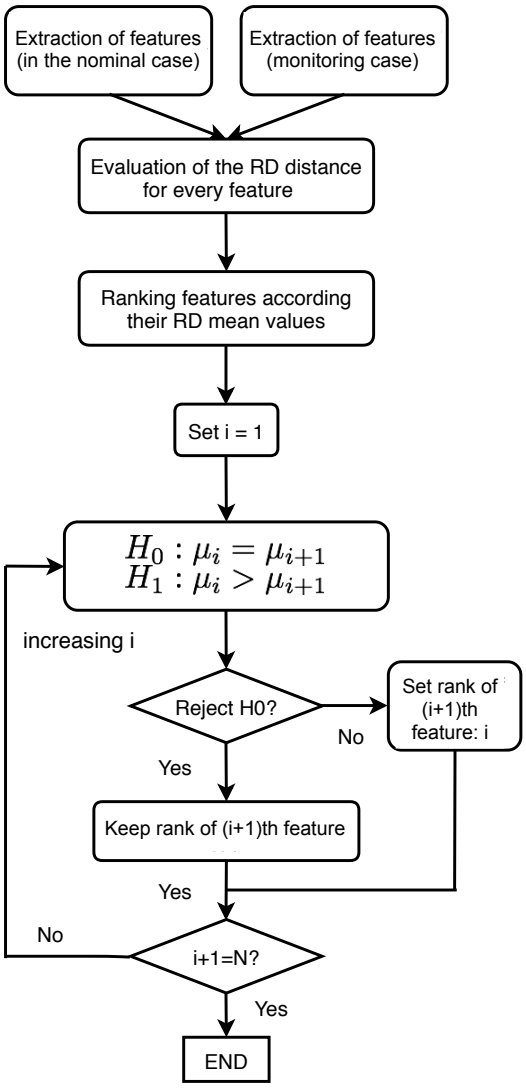

Figure 1. Feature ranking algorithm.

- being simple for prompt evaluation ;
- not depending on the feature units. Thus, it allows comparing heterogeneous features in different domains ;
- and taking into account the standard deviation of feature values when assessing their performance.

Therefore, we introduce in this section a measure, called the distance ratio (RD), that it is evaluated by the ratio between the Euclidean distance from a feature value (point i), extracted from a monitoring signal, to the median value of the set of nominal feature values (S_{FV}), characterizing the healthy state, and the standard deviation of nominal feature value set, $\sigma(S_{FV})$:

$$RD = \frac{||i - \text{median}(S_{FV})||_2}{\sigma(S_{FV})} \tag{1}$$

For fault detection and prognostics, if the extracted feature allows clearly distinguishing the normal and abnormal state,

then the feature performance is well highlighted. Considering Eq.1, if the distance of a feature value to the median value of the healthy state is significant while the standard deviation of distances between nominal feature values is small, then the corresponding RD is high. In other words, the greater RD value is, the higher feature performance will be. Therefore, RD can be used as an effective measure for feature performance ranking when considering fault detection and prognostic issues.

3.2. Feature ranking algorithm

To assess the feature robustness, it is essential to evaluate multiple RD measures corresponding to feature values extracted from numerous signal sources (for example, same signal type but different sensor positions). Therefore, in this subsection, a new algorithm of feature ranking, illustrated by Figure 1, is developed. This algorithm is based on the following principle: *the higher RD mean value of a feature is, the greater performance of this feature will be*. In detail, for ranking of N features, the RD measures are firstly evaluated for every feature. Then, N features are sorted according to their RD mean values such as the RD mean value of i-th feature is greater than the one of $i+1$-th feature ($\mu_i > \mu_{i+1}$). Next, it is necessary to verify the confidence level of this feature ranking list. In other words, we consider whether the results ($\mu_i > \mu_{i+1}$, $i \in [1, N-1]$) are statistical significant or only random observations.

- If $H_0 : \mu_i = \mu_{i+1}$ is rejected, the rank of i and $(i+1)$-th feature are maintained.
- If not, we can not conclude that the i-th feature is better than the $(i+1)$-th one. Consequently, they have the same rank.

4. EXPERIMENTAL VALIDATION

4.1. Description of the Experimental Setup

The test bench, performed on the PRIMES platform, aims to track the health state of the traction auxiliary motors in a train, particularly that one of their bearings, in order to plan the maintenance interventions. Figure 2 presents a general view of the experimental system configuration. In detail, a three-phase induction motor is powered via an onboard inverter. The motor can run at high speed (HS: 2880 rpm) or low speed (LS: 1440 rpm). It includes two bearings at the two ends: one with a load like a fan or a centrifugal pump, called drive end (DE) and the opposite side, named non drive end (NDE). In this paper, we will consider, in priority, the detection of the outer bearing fault, which is represented by a groove, created using the Electro Discharge Machining (EDM) technique: the diameter of the grove is 3 mm on the bearing outer race at the NDE. The data acquisition procedure is performed by a CompactRIO 9039 which also allows running the fault detection algorithms in real time and controlling the electrical machines from the LABVIEW software. In order to assess the performance and robustness of multiple features with different sensor placements, 4 accelerometers are mounted horizontally and vertically on the DE and the NDE of the motor to capture the vibration signals. On the other hand, the electrical signals provided by the on-board inverter are also measured and recorded through 6 current sensors (3 sensors for HS and 3 sensors for LS). For the healthy (or faulty) state, the collected data are composed of a) 200 samples of 1 s with a sampling frequency of 51.2 kHz for vibration signals, and b) 200 samples of 1 s with a sampling frequency of 50 kHz for current signals. Considering the bearing outer race defect, When the motor runs at the high speed, its corresponding characteristic frequency from the vibration signals is 171 Hz and the one from the current signals is $50 \pm k \times 171$ Hz (see Annex for the evaluation of characteristic frequencies).

Signal Processing methods	Features
Time domain	
Overall form	PP, IF, SF
Statistic evaluation	RMS, SKE, KUR, $THIKAT, TALAF$
Frequency domain	
Fast Fourier Transform	$BPFO$
Envelope analysis	$EBPFO$
Time-Frequency domain	
Wavelet Transform	$WT.O$
Hilbert Huang Transform	$HTT.O$

Table 1. Summary of extracted features.

Note that: PP: Peak to Peak, IF: Impulse Factor, SF: Shape Factor, RMS: Root mean square, SKE: Skewness, KUR: Kurtosis, $THIKAT, TALAF$ (Sassi et al., 2006),
$BPFO$: FFT Magnitude at outer race defect frequency f_o,
$EBPFO$: Envelope Amplitude at f_o,
$WT.O$: FFT Magnitude of Wavelet Transform coefficients at f_o,
$HHT.O$: HHT Marginal spectrum at f_o.

4.2. Discussion of feature performance

In time, frequency and time-frequency domains, we only focus on the features that are widely used for bearing fault detection and prognostics and easily extracted from both vibration and current signals. Table 1 summarizes 12 extracted features. The extraction procedure details of these features will be presented in the Annex.

In order to ensure the objectivity and robustness of the analyzed results corresponding to sensor positions, 200 samples of 1 s of vibration signals (or current signals) from accelerometers (or current sensors) and used to assess the features performance. In detail, 50 successive samples of 1 s are recorded from every sensor during 50 s. Figure 3 presents the box plot of the RD measures of time features extracted from vibration and current signals acquired by different accelerometers and current sensors. In general, the time features are effective for bearing outer fault (BOF) detection when using vibration signals. Indeed, the distance between

Features	Mean	SD	Rank	p-value(%)
$HHT.O$	225.88	47.89	1	0
PP	51.81	8.86	2	0
$WT.O$	39.04	19.71	3	1.1
$BPFO$	34.69	18.29	4	31
RMS	34.04	2.68	4	0
$EBPFO$	26.62	19.89	6	0
SKE	16.94	8.8	7	0
SF	5.32	2.69	8	0
$THIKAT$	3.89	1.75	9	2
KUR	3.48	2.19	10	17.7
IF	3.29	1.77	10	0
$TALAF$	0.86	0.32	12	

Table 2. Feature ranking for vibration signals with confidence level of 97.5%, BOF, HS: 2880 rpm.

Features	Mean	SD	Rank	p-value(%)
$HHT.O$	132.22	70.93	1	0
$WT.O$	29.46	11.81	2	0
$BPFO$	24.68	12.11	3	0
$EBPFO$	16.76	10.34	4	0
$THIKAT$	3.94	2.4	5	0.1
PP	3.23	1.97	6	0
IF	2.49	0.29	7	2.4
RMS	2.24	1.76	8	0
$TALAF$	0.73	0.42	9	3.3
SF	0.68	0.04	9	0
SKE	0.34	0.13	11	0
KUR	0.23	0.01	12	

Table 3. Feature ranking for current signals with confidence level of 97.5%, BOF, HS: 2880 rpm.

the normal and BOF state is well recognized according to features PP, RMS and SKE. The RD measures are respectively $RD_{PP} \in [36.6, 68.47]$, $RD_{RMS} \in [31.2, 39.1]$ and $RD_{SKE} \in [0.4, 25.1]$. However, the time features are not useful for current signals. There are small differences between the healthy and faulty states that can be recognized as $RD_{PP} \in [1.8, 6.7]$, $RD_{THIKAT} \in [2.3, 8.3]$.

The RD measure box plot of frequency features extracted from vibration and current signals are illustrated in Figure 4. We find that both $BPFO$ and $EBPFO$ allow effectively distinguishing the normal and BOF states when using vibration and also current signals. In fact, the RD measure of features extracted from vibration signals are $RD_{BPFO} \in [8.7, 78.9]$, and $RD_{EBPFO} \in [5.2, 65.2]$ while the one extracted from current signals are $RD_{BPFO} \in [8.1, 61.5]$, and $RD_{EBPFO} \in [0.76, 46.1]$. On the other hand, a paradox result is recognized here. Indeed, the performance of extracted features (represented by RD measures) based on the envelope analysis is expected be higher than the one based on the FFT analysis. However, the experimental result shows an opposite conclusion. This result again illustrates the point of view that the envelope analysis performance strictly depends on the selection of the filter parameters. For further work, an optimization of the band-pass filter, for example the Kurtogram analysis, should be carefully considered.

Figure 5 presents the RD measure box plot of time-frequency features extracted from vibration and current signals. We find that the time-frequency features, in particular the $HHT.O$, extracted from both vibration and current signals are very effective for bearing outer race fault detection. They allow clearly distinguishing the normal and faulty states. In detail, the RD measure of the features extracted from the vibration signals are $RD_{WT.O} \in [10.14, 89.4]$ and $RD_{HHT.O} \in [121.2, 381.5]$ while the one extracted from current signals are $RD_{WT.O} \in [8.3, 61.4]$, and $RD_{HHT.O} \in [39.8, 240.9]$.

Next, the ranking list of the features extracted from vibration and current signals when considering the BOF are respectively presented in Tables 2 and 3. In these tables, the mean and standard deviation (SD) of the RD measure of every feature are respectively given in the second and third column. The feature ranks, which are evaluated based on the algorithm summarized in Figure 1, are presented in the fourth column. Finally, the last column shows the p-value of the comparison test of RD mean values between the considered feature with the next feature in the ranking list. For example, considering $THIKAT$ feature in Table 2, its relevant p-value is 2%. It characterizes the probability of false rejection of the null hypothesis $H_0 : \mu_{RD_{THIKAT}} = \mu_{RD_{KUR}}$. Considering the confidence level of 97.5%, the hypothesis $\mu_{RD_{THIKAT}} = \mu_{RD_{KUR}}$ will be rejected (because $2\% < 100 - 97.5\%$). In other words, the conclusion that the performance of the $THIKAT$ feature is better than the KUR feature is proven.

Considering Tables 2 and 3, we find that the feature based on the Hilbert Huang Transform ($HHT.O$) is the best one for BOF detection using both vibration and the current signals. Next, the ranks of the rest of features are trivially different in two tables. For example, the PP feature in time domain is very effective (ranked at 2nd) for the vibration signal but is only in intermediate rank (6th) for the current signal. In fact, features in time domain are not reliable for current signals. In this case, it is suitable to use features in time-frequency ($HHT.O, WT.O$) or frequency ($BPFO$, $EBPFO$) domain to capture the change of the signals. On the other hand, an interesting result shows that the RD mean values of all features extracted from vibration signals are generally greater than the ones extracted from current signals. That means, for BOF detection, the vibration signals are better than the current signals.

5. CONCLUSION

We have presented in this paper a new metric that allows assessing the performance of heterogeneous features in different domains for fault detection, diagnostics and prognostics.

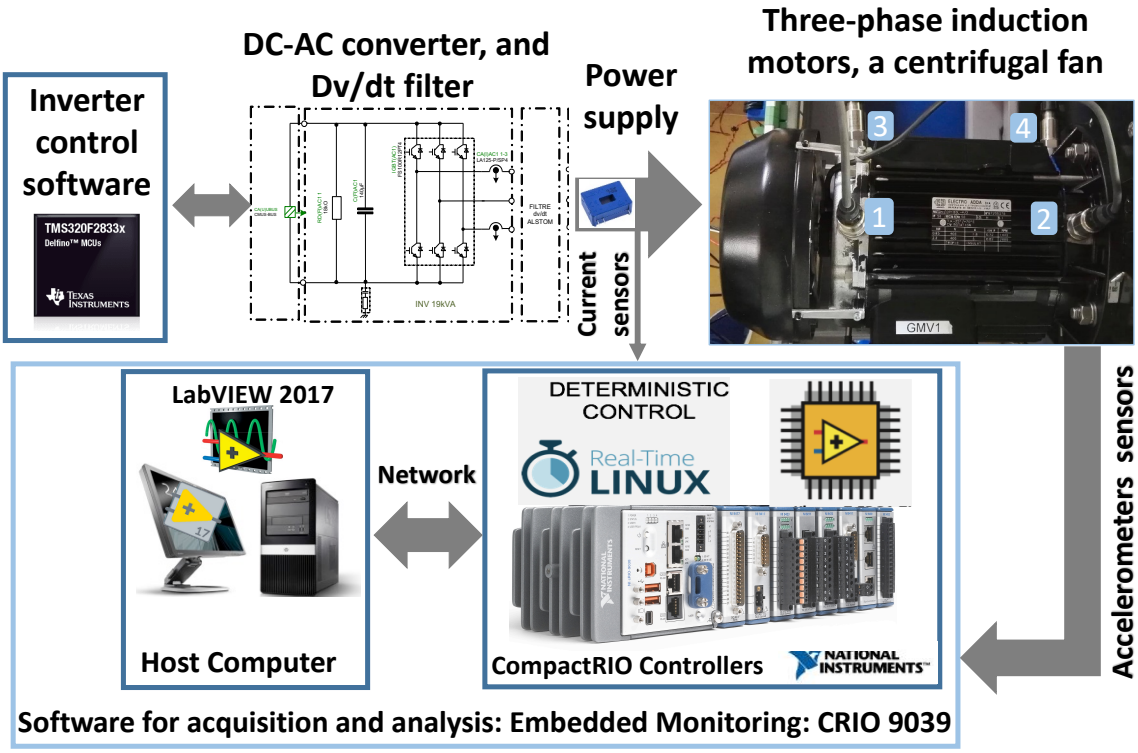

Figure 2. Experimental system configuration.

Based on this feature, a ranking algorithm is developed to study which features are better than others and which feature is the best effective from vibration or current signals. The algorithm was validated for the outer bearing fault detection based on real data acquired by various accelerometers and current sensors on a real test bench. An interesting result shows that, considering both vibration and current signals, among numerous features in time, frequency and time-frequency domains, the feature based on the Hilbert-Huang Transform, $HHT.O$, is the best one that allows clearly distinguishing the normal and outer bearing faulty states. However this feature requires a lot of time for its extraction and therefore should be improved for real time applications. On the other hand, the features in time domain are simply and rapidly extracted but are only useful when extracted from vibration signals. For current signals, it is suitable to use time-frequency or frequency features than the ones in time domain. This paper was focused, in priority, on the feature performance for detection of outer bearing fault. Further work should extend the study on different bearing localized and also distributed defects. The features robustness should be verified with different motor speeds et numerous diameter of groves on bearing. Moreover, a new powerful prognostic method based on the metric presented in this paper could be developed.

ACKNOWLEDGMENT

This work was performed in the framework of the "Predictive Maintenance R&D Auxiliary Motors" project. This project is part of collaboration between ALSTOM, LGP et LAPLACE. It is within a context of the Health Hub program that is launched by ALSTOM in order to develop dedicated technology for condition based maintenance and prognostics and health management (PHM).

ANNEX

Characteristic frequencies

For vibration signals, the characteristic frequencies associated to different types of bearing fault are evaluated as follows, (Shah & Patel, 2014):

- Outer race defect, $f_o = \frac{n}{2} f_r \left(1 - \frac{B}{D\cos(\alpha)}\right)$ where $n =$ number of balls in rolling element bearing, $B =$ ball diameter, $D =$ bearing pitch diameter, $\alpha =$ bearing contact angle and $f_r =$ rotor frequency.

These abnormal vibrations also generate rotating eccentricities or load torque variations. They lead to periodical changes in machines inductances and therefore deduce additional characteristic frequencies in the stator current f_c^s, (Schoen et al., 1994 ; Blodt et al., 2008).

- Considering the radial movement of the rotor center, the characteristic frequencies of current signals, f_c^s, are evaluated by following expressions:
  - Outer race defect, $f_o^s = f_s \pm k f_o$ where $f_s =$ electrical stator supply frequency, $f_r =$ rotor frequency and $k = 1, 2, 3, ...$

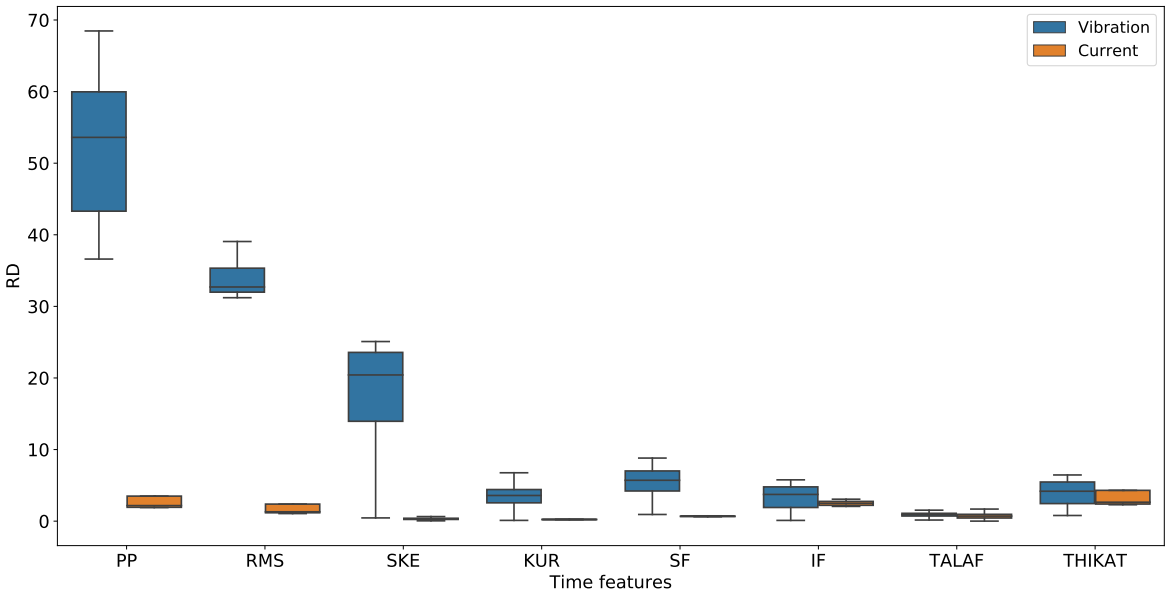

Figure 3. Comparison of features in time domain, BOF, HS: 2880 rpm.

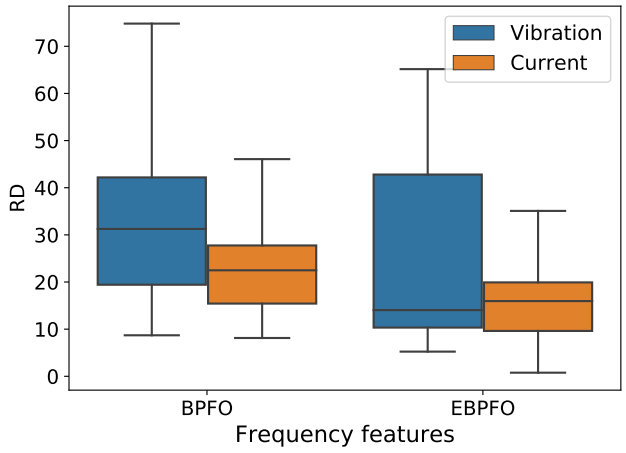

Figure 4. Comparison between features in frequency domain, BOF, HS: 2880 rpm.

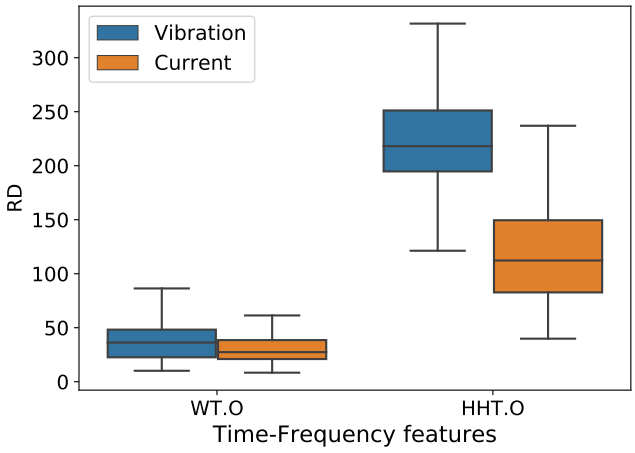

Figure 5. Comparison between features in time-frequency domain, BOF, HS: 2880 rpm.

- Considering the torque variation, the characteristic frequencies of current signals, f_c^s are given by:
  - Outer race defect, $f_o^s = f_s \pm k f_o$.

Evaluation of features

- In time domain, where $s(t_i)$ be the signal at time t_i:
  - Peak to Peak value (PP): $PP = |\max_i(s(t_i)) - min(s(t_i)|$
  - Root mean square value (RMS): $RMS = \sqrt{\frac{1}{n}\sum_i^n s(t_i)^2}$
  - Skewness value (SKE): $SKE = \frac{1}{n}\frac{\sum_i^n (s(t_i)-S_{mean})^3}{\sigma^3}$
  - Kurtosis value (KUR): $KUR = \frac{\frac{1}{n}\sum_{i=1}^n (s(t_i)-S_{mean})^4}{\left(\frac{1}{n}\sum_{i=1}^n (s(t_i)-S_{mean})^2)\right)^2}$
  - Shape factor value (SF): $SF = \frac{RMS}{S_{mean_abs}}$
  - Impulse factor value (IF): $IF = \frac{\max_i(s(t_i))}{S_{mean_abs}}$
  - TALAF value: $TALAF = log\left(KUR + \frac{RMS}{RMS_0}\right)$ where RMS_0 is the RMS value defined for a healthy bearing at the initial moment.
  - THIKAT value: $THIKAT = log\left(KUR^{CF} + \left(\frac{RMS}{RMS_0})\right)^P\right)$ where CF is the crest factor, $CF = \frac{P}{RMS}$ and P is the peak value of signals, $P = \max_i(s(t_i))$
- In frequency domain:
  - $BPFO$: FFT Magnitude at outer race defect frequency f_o.
  - $EBPFO$: Envelope Amplitude at f_o, that is evaluated based on the envelope analysis:
    - Hilbert transform of signal ;
    - Calculation of the envelope signal $A(t)$: $A(t) = x_R^2(t) + x_I^2(t)$ where x_R and x_I are the real and image part of the Hilbert ;
    - Fast Fourier transform of the envelope signal and extraction of the amplitude at f_o.
- In time-frequency domain:
  - $WT.O$ is the FFT Magnitude of Wavelet Transform coefficients at f_o is evaluated as follow:
    - Discrete Packet Wavelet Transform of signals, (Knöbel et al., 2015) ;
    - Fast Fourier transform of all sub-signals ;
    - Extraction of the amplitude at f_o of all sub-signals ;
    - $WT.O$ is the maximal value of the magnitudes at f_o of sub-signals.
  - $HHT.O$ is the HHT Marginal spectrum at f_o, which is evaluated as follow:
    - Empirical mode decomposition of signals to obtain a collection of intrinsic mode functions (IMFs) ;
    - Evaluation of the marginal Hilbert spectrum of all IFMs at f_o, (Soualhi et al., 2015) ;
    - $HHT.O$ is the maximal value of the marginal Hilbert spectrum at f_o.

REFERENCES

Alameh, K., Cité, N., Hoblos, G., & Barakat, G. (2015, April). Feature extraction for vibration-based fault detection in Permanent Magnet Synchronous Motors. In *2015 Third International Conference on Technological Advances in Electrical, Electronics and Computer Engineering (TAEECE)* (pp. 163–168).

Blodt, M., Granjon, P., Raison, B., & Rostaing, G. (2008, April). Models for Bearing Damage Detection in Induction Motors Using Stator Current Monitoring. *IEEE Transactions on Industrial Electronics*, *55*(4), 1813–1822.

Cong, F., Chen, J., & Dong, G. (2012, February). Spectral kurtosis based on AR model for fault diagnosis and condition monitoring of rolling bearing. *J Mech Sci Technol*, *26*(2), 301–306.

Deekshit Kompella, K. C., Venu Gopala Rao, M., & Srinivasa Rao, R. (2017, July). Bearing fault detection in a 3 phase induction motor using stator current frequency spectral subtraction with various wavelet decomposition techniques. *Ain Shams Engineering Journal*.

Elbouchikhi, E., Choqueuse, V., Amirat, Y., Benbouzid, M. E. H., & Turri, S. (2017, June). An Efficient Hilbert Huang Transform-Based Bearing Faults Detection in Induction Machines. *IEEE Transactions on Energy Conversion*, *32*(2), 401–413.

E. Fournier, A. Picot, J. Régnier, M. TientcheuYamdeu, J.M. Andréjak, and P. Maussion. (2015). Current-based Detection of Mechanical Unbalance in an Induction Machine Using Spectral Kurtosis with Reference. *Industrial Electronics, IEEE Transactions on*, *62*(3), 1879–1887.

Ghods, A., & Lee, H.-H. (2016, May). Probabilistic frequency-domain discrete wavelet transform for better detection of bearing faults in induction motors. *Neurocomputing*, *188*, 206–216.

Harlişca, C., Szabó, L., Frosini, L., & Albini, A. (2013, May). Diagnosis of rolling bearings faults in electric machines through stray magnetic flux monitoring. In (pp. 1–6).

Huang, Z., Xu, Z., Ke, X., Wang, W., & Sun, Y. (2017, March). Remaining useful life prediction for an adaptive skew-Wiener process model. *Mechanical Systems and Signal Processing*, *87*, 294–306.

Kappaganthu, K., & Nataraj, C. (2011, September). Feature Selection for Fault Detection in Rolling Element Bearings Using Mutual Information. *J. Vib. Acoust*, *133*(6), 061001–061001–11.

Knöbel, C., Marsil, Z., Rekla, M., Reuter, J., & Gühmann, C. (2015, August). Fault detection in linear electromagnetic actuators using time and time-frequency-domain features based on current and voltage measurements. In *2015 20th International Conference on Methods and Models in Automation and Robotics (MMAR)* (pp. 547–552).

Kompella, K. C. D., Mannam, V. G. R., & Rayapudi, S. R. (2016, December). DWT based bearing fault detection in induction motor using noise cancellation. *Journal of Electrical Systems and Information Technology*, *3*(3), 411–427.

Lei, Y., Li, N., & Lin, J. (2016, December). A New Method Based on Stochastic Process Models for Machine Remaining Useful Life Prediction. *IEEE Transactions on Instrumentation and Measurement*, *65*(12), 2671–2684.

Leite, V. C. M. N., Silva, J. G. B. d., Veloso, G. F. C., Silva, L. E. B. d., Lambert-Torres, G., Bonaldi, E. L., & Oliveira, L. E. d. L. d. (2015, March). Detection of Localized Bearing Faults in Induction Machines by Spectral Kurtosis and Envelope Analysis of Stator Current. *IEEE Transactions on Industrial Electronics*, *62*(3), 1855–1865.

Mahamad, A. K., & Hiyama, T. (2008, December). Development of artificial neural network based fault diagnosis of induction motor dearing. In *2008 IEEE 2nd International Power and Energy Conference* (pp. 1387–1392).

Refaat, S. S., Abu-Rub, H., Saad, M. S., Aboul-Zahab, E. M., & Iqbal, A. (2013, February). ANN-based for detection, diagnosis the bearing fault for three phase induction motors using current signal. In *2013 IEEE International Conference on Industrial Technology (ICIT)* (pp. 253–258).

Sassi, S., Badri, B., & Thomas, M. (2006). TALAF and THIKAT as innovative time domain indicators for tracking BALL bearings. In *CMVA: Proceedings 24th seminar on machinery vibrartion.* (pp. 404–419).

Schoen, R. R., Habetler, T. G., Kamran, F., & Bartheld, R. G. (1994, October). Motor bearing damage detection using stator current monitoring. In *Proceedings of 1994 IEEE Industry Applications Society Annual Meeting* (pp. 110–116 vol.1).

Shah, D. S., & Patel, V. N. (2014, January). A Review of Dynamic Modeling and Fault Identifications Methods for Rolling Element Bearing. *Procedia Technology*, *14*, 447–456.

Shukla, S., Yadav, R. N., Sharma, J., & Khare, S. (2015, December). Analysis of statistical features for fault detection in ball bearing. In *2015 IEEE International Conference on Computational Intelligence and Computing Research (ICCIC)* (pp. 1–7).

Singh, S., Kumar, A., & Kumar, N. (2014, January). Motor Current Signature Analysis for Bearing Fault Detection in Mechanical Systems. *Procedia Materials Science*, *6, Supplement C*, 171–177.

Soualhi, A., Medjaher, K., & Zerhouni, N. (2015, January). Bearing Health Monitoring Based on Hilbert Huang Transform, Support Vector Machine, and Regression. *IEEE Transactions on Instrumentation and Measurement*, *64*(1), 52–62.

Tandon, N. (1994, January). A comparison of some vibration parameters for the condition monitoring of rolling element bearings. *Measurement*, *12*(3), 285–289.

Tobon-Medjia, D.A., Medjaher, K. , Zerhouni, N. , Tripot, G. (2012, June). A Data-Driven Failure Prognostics Method Based on Mixture of Gaussians Hidden Markov Models. *IEEE Transactions on Reliability*, *61*(2), 491–503.

Yazici, B., & Kliman, G. B. (1999, March). An adaptive statistical time-frequency method for detection of broken bars and bearing faults in motors using stator current. *IEEE Transactions on Industry Applications*, *35*(2), 442–452.

Yu, J. (2012, May). Local and Nonlocal Preserving Projection for Bearing Defect Classification and Performance Assessment. *IEEE Transactions on Industrial Electronics*, *59*(5), 2363–2376.

Zhou, W., Habetler, T. G., & Harley, R. G. (2007, September). Bearing Condition Monitoring Methods for Electric Machines: A General Review. In *2007 IEEE International Symposium on Diagnostics for Electric Machines, Power Electronics and Drives* (pp. 3–6).